ISSN 0001-4370, Oceanology, 2021, Vol. 61, No. 6, pp. 791–802. © Pleiades Publishing, Inc., 2021.
Russian Text © The Author(s), 2021, published in Okeanologiya, 2021, Vol. 61, No. 6, pp. 856–868.

MARINE PHYSICS

Effect of the East Siberian Current on Water Exchange in the Bering Strait Based on Satellite Altimetry Measurements

V. R. Zhuk[a, b, *] and A. A. Kubryakov[a]

[a] *Marine Hydrophysical Institute, Russian Academy of Sciences, Sevastopol, Russia*
[b] *Sevastopol State University, Sevastopol, Russia*
**e-mail: zhuk.vladislav@ya.ru*

Received December 7, 2020; revised March 12, 2021; accepted April 8, 2021

Abstract—The seasonal and interannual variability of water exchange in the Bering Strait and its relationship with Arctic circulation is investigated on the basis of satellite-altimetry measurements between 1993 and 2016. The intensification of northern currents in the strait is observed from April to August, when their mean speed is approximately 25 cm/s. During September–November, a sharp weakening of the speed is observed, and in some years, there is even a change in the current direction to the south with monthly average speeds of up to 10 cm/s. Two pronounced minima have been recorded on the interannual scale in the intensity of northern currents in 2002–2003 and 2012–2013. These minima are associated with strengthening of the East Siberian Current (also known as the Siberian Coastal Current), which in some years extends far to the east and flows into the Bering Strait. As a result, a southern current appears in the western part of the strait, which partially blocks the flow of Pacific waters into the Arctic. The bi-directional structure of currents is observed from satellite temperature measurements, which record the flow of cold Arctic waters into the strait in autumn. Studies of the relationship between water exchange and the wind field show that intensification of the northwestern winds, north of the New Siberian Islands, causes intensification of the East Siberian Current, which apparently leads to an increase in the eastern transport of waters from the Laptev Sea.

Keywords: Bering Strait, satellite altimetry, water exchange, East Siberian Current, seasonal and interannual variability, Chukchi Sea, Pacific waters

DOI: 10.1134/S0001437021060175

1. INTRODUCTION

The Chukchi Sea is the gateway between the Pacific and Arctic oceans. Currents in this marginal sea play an important role in the formation of the hydrological characteristics of the Eastern Arctic. The transport of Pacific waters through the Bering Strait into the Chukchi Sea is about 30000 km^3 [2]. The inflow of the Pacific Ocean's saline waters significantly affects the salt balance and salinity structure of the Arctic [1, 26], largely determining the features of its dynamics, in particular, the intensity of anticyclonic circulation in the Pacific sector of the Arctic (Beaufort Gyre) [1, 26]. In summer and early autumn, warmer flows through the Bering Strait contribute to both ice melting and the retention of pack ice in the Chukchi Sea [20]. In addition, the Pacific waters are the most important source of nutrients and their input significantly affects the ecosystem of the Chukchi Sea and the Eastern Arctic as a whole [22].

The flow of water from the Bering Strait, its interannual variability, and its physical causes were investigated in a large number of works based on contact measurements including data from mooring buoys [6, 25–27], and numerical modeling [3, 8, 14, 19]. However, most of these works are concentrated in the American (eastern) sector of the strait [6, 25, 26, 30]. At the same time, there are very few data on the dynamics of currents in the Eurasian sector of the strait. The result of the joint Russian-American experiment RUSALCA is an exception [27]. Studies of currents in the strait based on oceanographic measurements, acoustic doppler current profiler (ADCP) data, and mooring buoys show that geostrophic currents associated with a sharp salinity gradient between the eastern and western parts of the strait make a significant contribution to the transport of water through the strait. Thus, with a certain accuracy, the flow rates in the strait can be estimated using the geostrophic approximation, according to [7, 26, 27].

The opinions of researchers also differ on the main factors determining the intensity of flows through the Bering Strait. Most researchers historically associate this variability with the effect of the wind directly over the strait, the variability of which is determined by the rearrangement of large-scale atmospheric fields [9, 25, 26, 28, 29] and forms a pressure difference in the strait [28, 29]. It was believed that the dynamics of the Pacific Ocean, where the variability of the northerly winds determines the intensity of the flow of Pacific

waters, has a decisive influence on the transport of waters through the strait [9].

At the same time, in recent work [14], the authors showed on the basis of gravimetric data from the GRACE satellite that the dynamics of the East Siberian Sea, which forms the level field north of the strait, has a major influence on these flows. These results demonstrated for the first time the significant influence of Arctic circulation on water exchange with the Pacific Ocean. Later, these results were confirmed by model calculations [13], in which the authors indicate that atmospheric circulation over the East Siberian Sea has an important effect on transport across the strait over large time scales. The authors also suggested that shelf waves propagating from the East Siberian Sea are the main factors influencing the dynamics of the strait. Thus, at present, assumptions about the mechanisms of the influence of wind and Arctic circulation on the variability of flows through the Bering Strait differ.

Modern altimetry data provide regular information on sea-surface height fields and geostrophic currents in the ocean and provide additional information on the spatial and temporal variability of the dynamics of the Arctic seas. A number of researchers show that the geostrophic component of velocity plays an important role in the variability of currents in the Bering Strait [7, 26, 27], which makes it possible to use altimetry data to assess the variability of flows in the sea. These data were first used to assess transport through the Bering Strait in [7]. However, the main conclusions of this work do not address the impact of Arctic dynamics on the flow of Pacific waters, the importance of which has been shown in more recent studies [13, 14]. In addition, a larger time range of data has become available, which can supplement the available information. Altimetry measurements were also used in recent works to study the features of currents in the pre-strait zones and in the central part of the Bering Sea [5, 15] and their influence on the transport of impurities.

In this work, we for the first time investigate the interannual variability of water exchange in the Bering Strait based on the analysis of altimetry data for more than 20 years (1993–2016) and its relationship with the Arctic circulation and wind characteristics. It is shown for the first time on the basis of data analysis that intensification of the East Siberian Current in specific years leads to its penetration into the Bering Strait, which contributes to blocking water exchange through the strait and significantly affects the flow of Pacific waters into the Arctic.

2. DATA

In our study we used mapped altimetry data on absolute dynamic topography and geostrophic velocities in the eastern sector of the Arctic between 1993 and 2016. The data was obtained from the Copernicus Marine Environment Monitoring Service portal (product SEALEVEL_GLO_PHY_L4_REP_OBSERVATIONS_008_047). The spatial resolution of the mapped data is 0.25° and the time resolution is one day. Thus, all conclusions about the current velocity in this work are related exclusively to its geostrophic component.

This region is characterized by the presence of ice, especially in winter, but if ice gets into the satellite measurement spot, the data are filtered out [10]. Validation of the altimetry data in the Arctic was also carried out in [21], in which it was shown that altimetry is able to describe well the variability of the sea-surface height in the Arctic regions, including the coastal zone; it is consistent with the data of coastal stations. In the same work, it was shown that altimetry data make it possible to describe synoptic fluctuations in the current velocity in the Arctic regions, the estimates of which are consistent with the data of drifters. The applicability of along-track altimetry data for describing water transport in the Bering Strait was demonstrated in a number of previous works [7, 29] based on comparison with direct mooring measurements and ADCP data. In these works, it was shown that a significant part of the currents in the strait can be described using the geostrophic approximation [27].

The mapped data were obtained from combined measurements of the along-track altimetry measurements. The initial resolution of the along-track altimetry data is about 7 km (see https://resources.marine.copernicus.eu/?option=com_csw&view=details&product_id=SEALEVEL_GLO_PHY_L3_REP_OBSERVATIONS_008_062). At the same time, we note that convergence of the satellite tracks occurs at high latitudes, i.e., the number of measurements increases, which leads to more accurate altimetry-level maps. The largest number of satellite tracks with altimeters and their highest resolution are observed in the Bering-Strait region at 66° N, because the inclination angle of the orbit of the TOPEX/Poseidon and Jason satellites series is 66° (see Fig. 3 in [7] with the distribution of TOPEX/Poseidon tracks). In the strait region, there are about seven altimetry tracks, each of which has 18 along-track measurements with a resolution of about 7 km. These were the latitudes that were used for analysis, which makes it possible to obtain altimetry data with the highest spatial and temporal resolution.

To estimate the total flux through the strait, in any case it is necessary to use averaging, which is applied used when obtaining a mapped array. In order to estimate possible errors in the mapped data, Fig. 1 shows a comparison of the variability of the meridional velocity component *Vy* at the 66° section using mapped and along-track data. The variability according to the along-track data was obtained by averaging the velocity at the points included in the region from 65.8° to 66.2° N and from 169°30′ to 167°30′ W. We

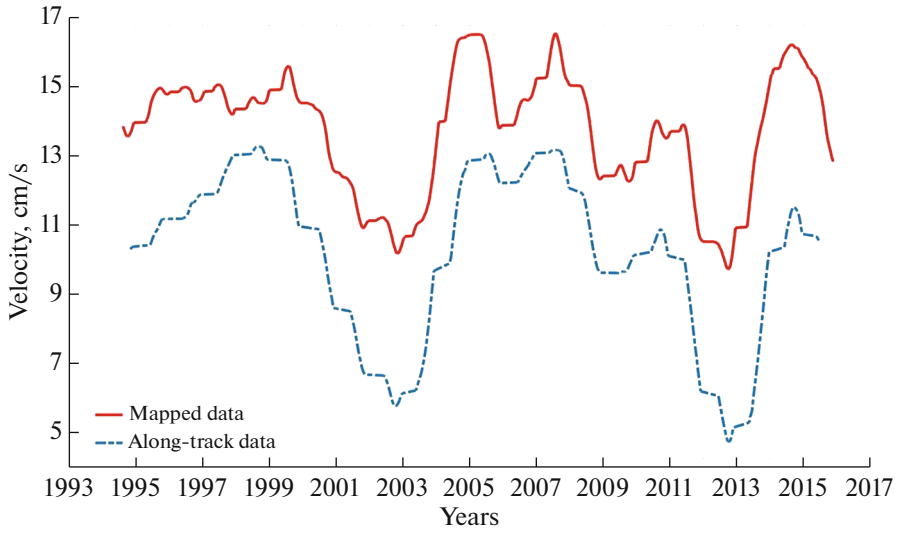

Fig. 1. Comparison of the variability of the meridional velocity component based on mapped (red line) and along-track (blue dotted line) data, smoothed by a 1-year running average (positive values are related to the northward direction of currents).

note that the absolute values slightly differ by a constant value of 2–3 cm. However, the main features of the variability are the same. In both series, a sharp weakening of the northern water flow was observed in 2002–2003 and 2012–2013 and there was intensification in other years (Fig. 1). The correlation between series smoothed by the 1-year running average is 0.95.

We note that along-track altimetry data are not available near the coast (at a distance of about 10 km (see [7]). Coastal currents in these zones can affect the estimates of the total flux. However, according to estimates [18, 26] based on contact measurements, the contribution of these currents to the total water exchange does not exceed 20% [7]. Thus, the mapped data used in this work are in good agreement with the along-track measurements, the applicability of which for describing flows through the strait was demonstrated in [7].

Information about the wind speed at a height of 10 m was obtained from MERRA reanalysis data at https://disc.gsfc.nasa.gov/datasets?project=MERRA. These are monthly wind-speed fields with a spatial resolution of 0.5° × 0.66°.

The work also used monthly maps of the ocean-surface temperature from measurements of the MODIS-Aqua (Level 3) scanner archive data (http://oceancolor.gsfc.nasa.gov/). The resolution of the sea-surface temperature maps is 4 km.

3. RESULTS

3.1. Variations in the Current Velocity in the Bering Strait

The mean field of currents in the region of the strait based on data on the mean dynamic topography (MDT) [16], and the diagram of the currents in the study site are shown in Fig. 2. The MDT field is determined based on a combination of all available oceanographic data, gravity measurements, and simulations [16, 17]. The data qualitatively coincide with the scheme of currents in [6], constructed on the basis of analysis of a number of hydrographic sections in [23]. In the strait, currents with a speed of 16 to 22 cm/s are generally directed northward. The Alaska Coastal Current with characteristic velocities from 14 to 20 cm/s directed to the northeast exists northwest of the strait. Part of the flow of the Pacific waters at 68°–69° N turns to the west forming a western branch in the Chukchi Sea. In the northeastern part of the strait, currents are directed eastward, reflecting the influence of the coastal East Siberian Current (also known as the Siberian Coastal Current).

We note that Fig. 2a and 2b agree qualitatively, but there are also some differences. For example, the East Siberian Current is not traced in Fig. 2a. As is known from a number of works [12, 24, 27], the East Siberian Current is quasi-constant and may be absent in the mean field of currents near the eastern coast of the strait. The diagram in Fig. 2 is constructed on the basis of several hydrographic sections in the entire study site of the Arctic, only a small part of which affects the Eurasian sector of the Arctic and reveals only a qualitative pattern of currents prepared subjectively by the authors of [6]. Due to the relatively low resolution of gravimeters and the small amount of data in the Chukotka sector, the altimetry data may also contain errors.

To study the flows through the Bering Strait using altimetry data, we analyzed the variability of the y component of velocity *Vy* over the section along 66° N (purple line in Fig. 2a). Figure 3 shows the average seasonal variability of the *Vy* distribution over longitudes during 1993–2016. Despite the fact that during the cold period the strait is often covered with ice, in

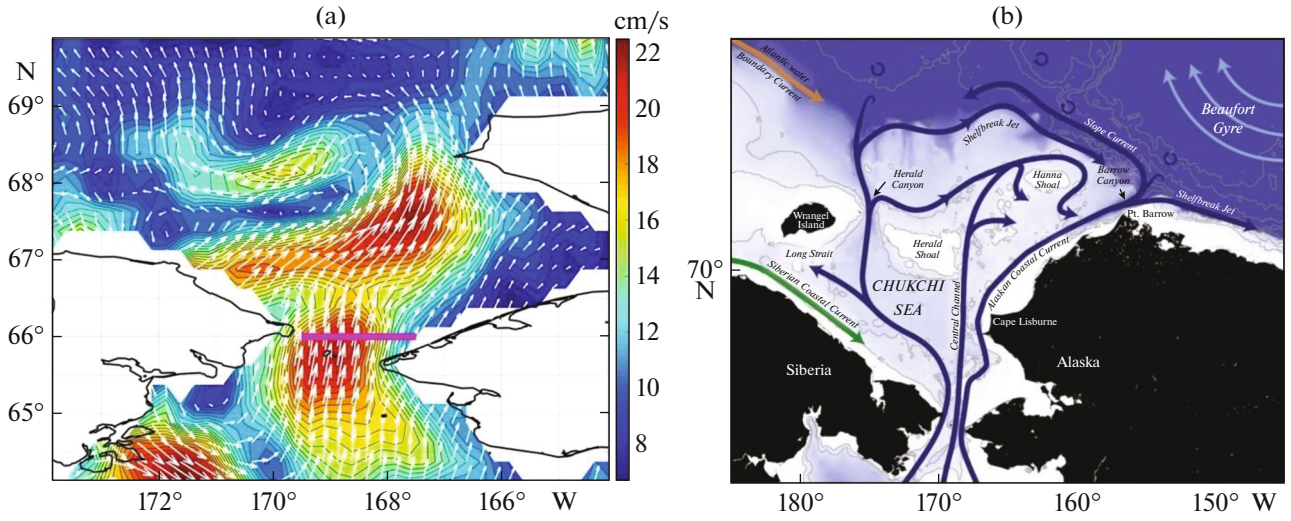

Fig. 2. Mean velocities of currents in the region of the strait between 1993 and 2016. The purple line shows the section for the analysis of transport through the Bering Strait (a). Circulation diagram of the Chukchi Sea from [6] (b). The diagram is used with the permission of the authors.

some years altimetry data are available also in the winter season (see Fig. 4b). This has become especially frequent in recent years (2014–2016), which is associated with observed global warming. Thus, one has to take into it account that in the presented diagram, the winter values were obtained only during very warm years (see Fig. 3b).

It is seen from the analysis that the highest velocities are found in the part of the strait from 169°30′ to 168°30′ W. The velocity in this region does not fall below 16 cm/s, except for September–November, when it reaches its minimum values, which range from 8 to 10 cm/s. The most intense flow of Pacific waters into the Chukchi Sea is observed from early April to early September, when their speed reaches 25 cm/s. The second maximum is recorded from January to February with mean speeds up to 18 cm/s. The eastern part of the strait (168°30′–167°37′ W) is characterized by the minimum speeds, which range from 4 to 10 cm/s with a minimum in September–November. These estimates are consistent with the analysis of measurements on mooring buoys [25, 26], which also showed an increase in the flow in the summer season and a decrease between October and December.

Figure 4a shows the time variability of the meridional velocity averaged over longitudes (positive values are related to the northern component of currents). Analysis shows that there are strong velocity variations in the strait. The velocity values vary widely from –34 to 41 cm/s. These changes have a pronounced seasonal course. The highest velocities (of northern currents) are observed in summer (20–40 cm/s), then a weakening of *Vy* is observed, and in late autumn, southern currents with velocities from 10 to 33 cm/s are often recorded.

Figure 4b shows a diagram of the interannual variability of the monthly mean northern velocity component. We note the rather high intra-annual and interannual variability. The highest velocities prevail in the summer season from June to August, they range within 15–25 cm/s. Peak values (exceeding 25 cm/s) are recorded in some years both in May (1998) and in September (2007), but most often they are observed in July and August. The minimum speed is observed in the autumn period. It is noteworthy that in October and November, the current in some years (2001, 2002, 2003, 2009, and 2012) changes direction to the south with monthly mean velocities from 4 to 12 cm/s.

The interannual variability of the *Vy* component averaged over the section in the Bering Strait for the series smoothed by the 1-year running average is shown in Fig. 5 (blue line). The annual mean speed varies from 9.7 to 16.5 cm/s. The maximum values were recorded in 2004, 2007, and 2014. The most pronounced feature of this variability is the periods of sharp weakening of flows through the Bering Strait. Such phenomena were observed twice from 1993 to 2016: in 2002–2003 and in 2012–2013. During these periods, the average speed reached a minimum, up to 9.7 cm/s. A notable weakening was also observed in 2008–2010, up to about 12.3 cm/s.

3.2. Influence of Arctic Circulation on Water Flow Through the Bering Strait

The properties of currents are seen in more detail on the monthly mean maps for individual years. For example, Fig. 6 shows the maps of current velocities in July and October of the years of high (1999) and minimum (2002) values of *Vy*. In July 1999, intense north-

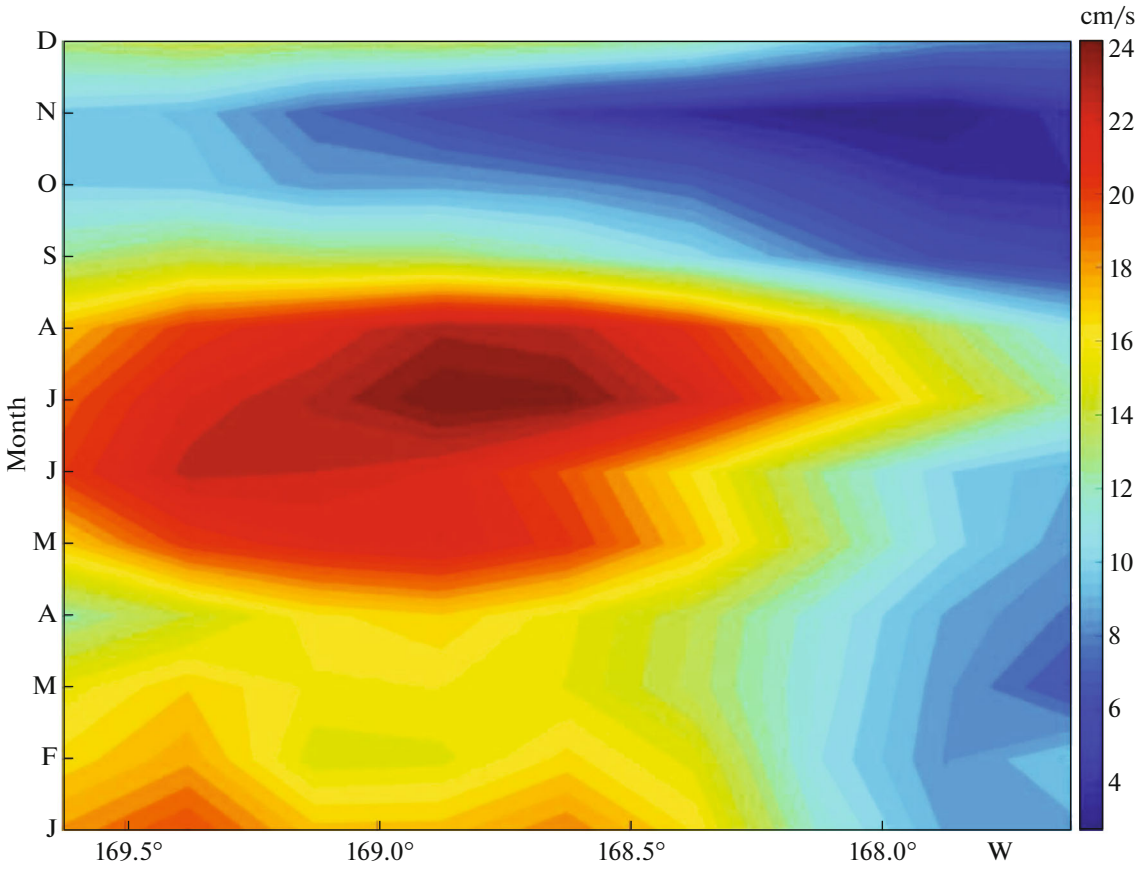

Fig. 3. Seasonal variability (mean 1993–2016) of the meridional component of the current velocity *Vy* across the Bering Strait over the section along 66° N.

ern velocities were observed over the entire width of the strait and reached 30 cm/s on average. High velocities of currents in the northern direction were recorded from 65° to 69° N. For comparison: in July 2002, the currents in the strait were much weaker and their velocities were about 15 cm/s. The northern flow of the Pacific waters in the Chukchi Sea was also much weaker.

During the seasonal minimum in October 1999, the width and intensity of the flow immediately in the strait decreased to 20 cm/s. To the north of the strait, the currents were directed to the east. In the eastern part of the strait, this flow turned to the south, forming an anticyclonic cell in the northern part of the strait.

An even more significant restructuring of currents was observed in October 2002. At this time, a strong current was observed to the northwest of the strait along the entire northern coast of the Chukchi Peninsula, the position of which corresponds to that of the coastal East Siberian Current (Fig. 2b). The speed of this current reached 25–30 cm/s. In the eastern part of the peninsula, this current turned to the south and flowed directly into the Bering Strait. Thus, satellite altimetry data indicate that in certain years intensification of the East Siberian Current leads to its flowing into the Bering Strait. As a result, a southern current appears in part of the strait, directed into the Bering Sea from the Arctic. Due to this, the width and total flow of Pacific waters into the Chukchi Sea are significantly reduced. As a result, the northern velocity component in the strait significantly decreases, which is reflected in the interannual variability of transport through the strait (Fig. 5).

It is known from previous studies that the East Siberian Current is quasi-constant and is capable of changing its direction from southeast to northwest [12, 24, 27]. These works show that generally, before reaching the Bering Strait, it separates from the coast and mixes with the surrounding waters, but infrequently it can flow into the strait. Figure 6 shows that altimetry data make it possible to observe this variability and determine the extent and intensity of the East Siberian Current.

The bi-directional structure of currents in the Bering Strait can be periodically clearly observed on the MODIS monthly average temperature maps. Clear traces of the flow of cold waters in the western part of the Chukchi Sea with temperatures 4–10°C lower than in the eastern part are seen in Fig. 7. It is likely that this water of Arctic origin often reaches the strait

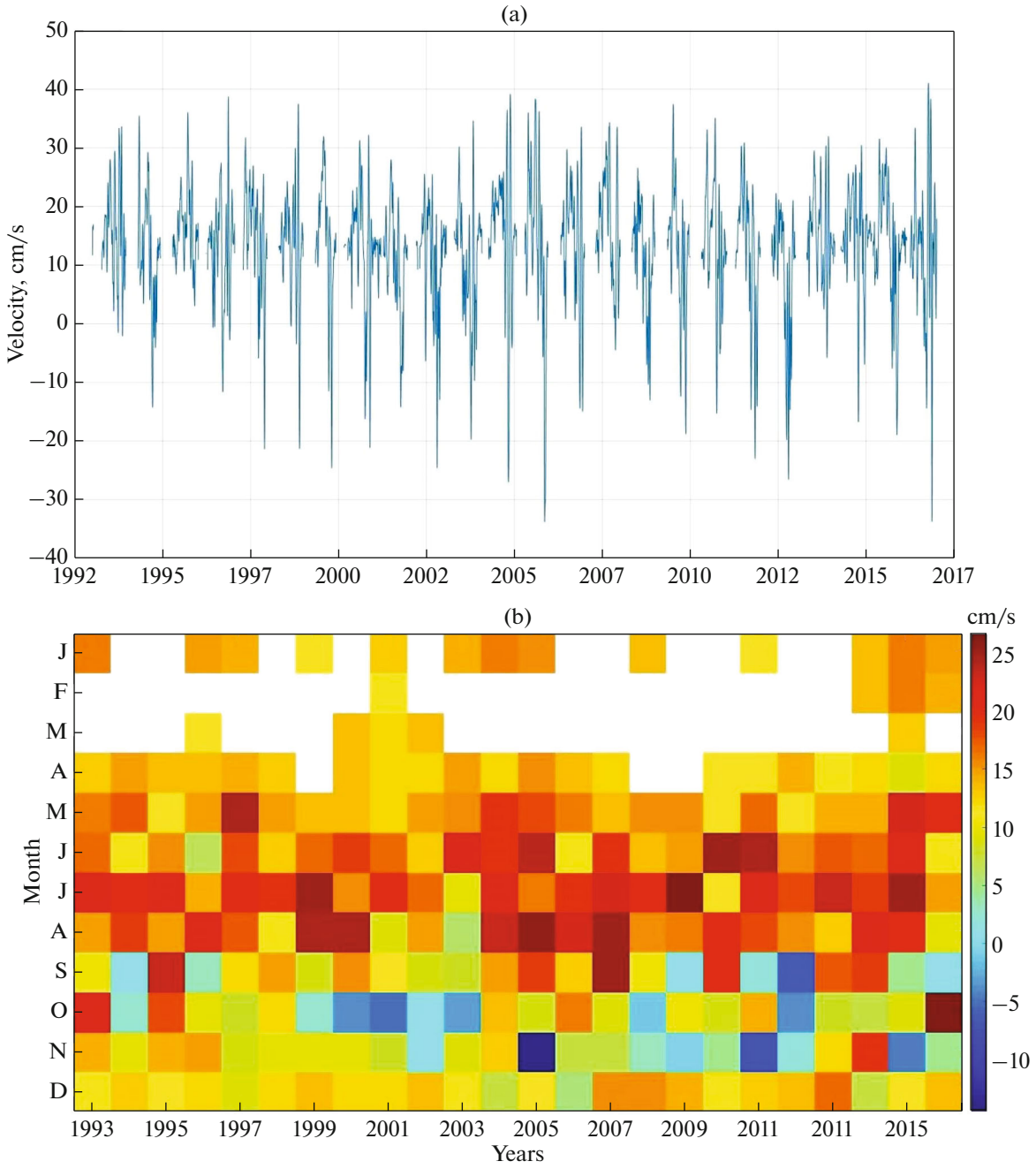

Fig. 4. Interannual variability of the velocity *Vy* (mean over the section along 66° N; positive values are related to the northern direction of currents) in the Bering Strait (a). Diagram of interannual variability of the mean monthly velocity component *Vy* (white color – no data) over the observation period (b).

and occupies from one third to one half of its width. In September 2012, the temperature in the western part of the strait was about 0–1°C, and in the eastern part it was warmer by 6–8°C. Most often, such penetration was observed in the autumn period in September–November, which is consistent with the altimetry data, but in some years (in 2001) it was also noted in August.

All these observations indicate the presence of a correlation between two opposing currents: the East Siberian Current to the northwest of the strait and the northern flow of the Pacific Ocean waters through the Bering Strait. Correlation analysis was used to investigate this relationship. The correlation coefficients were calculated between the mean meridional velocity through the Bering Strait and the

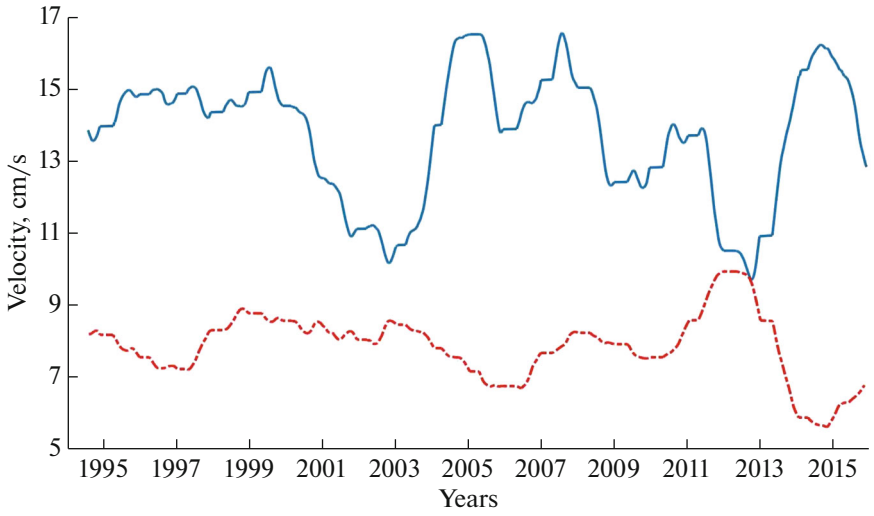

Fig. 5. Interannual variability of the current velocity in the Bering Strait (blue line) and current velocity *Vx* over the meridian section along 170°36′ W from 66°36′ to 67°38′ N (red dotted line) smoothed by a 1-year running average.

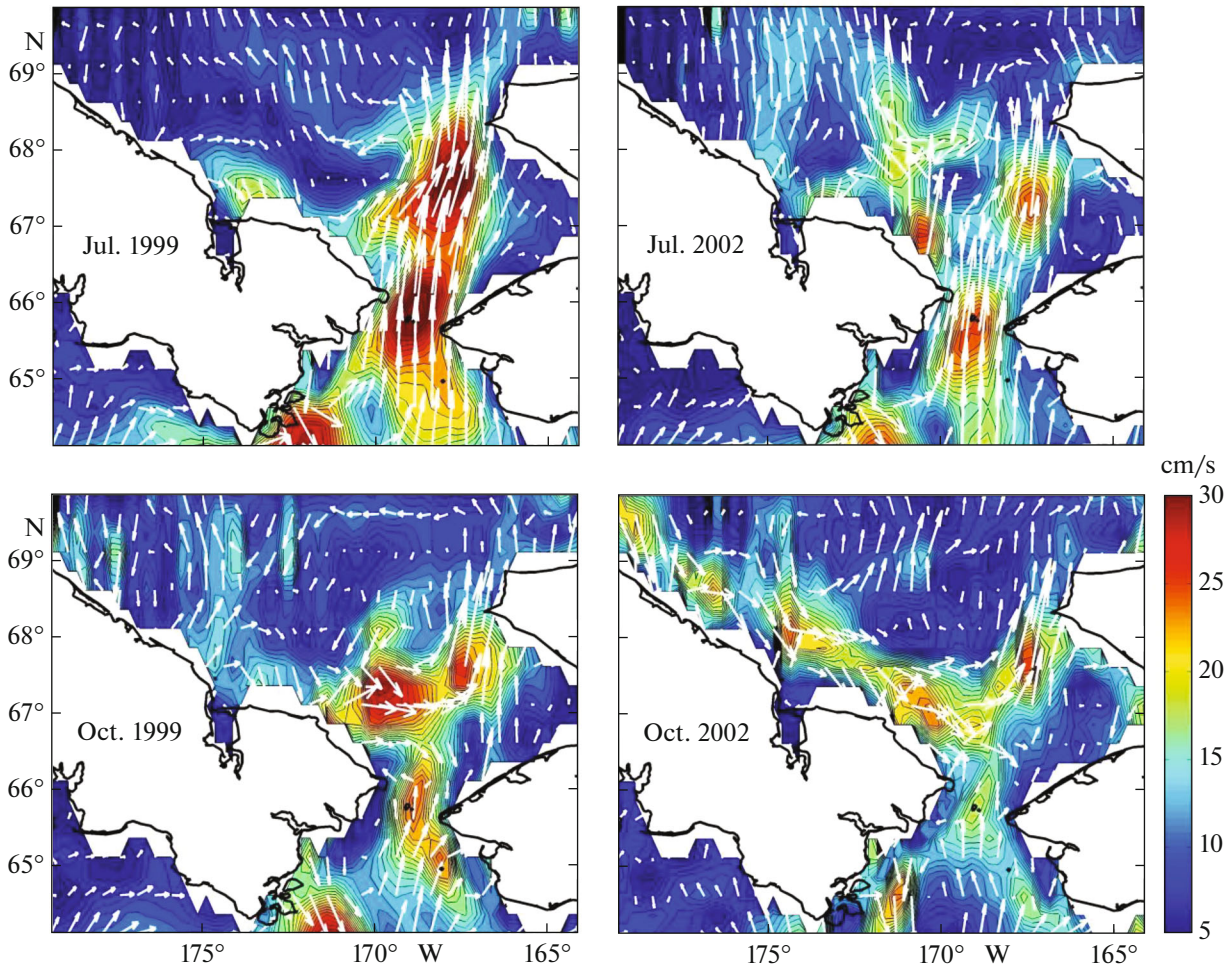

Fig. 6. Monthly mean maps of the velocity field of geostrophic currents in July and October 1999 (left) and 2002 (right).

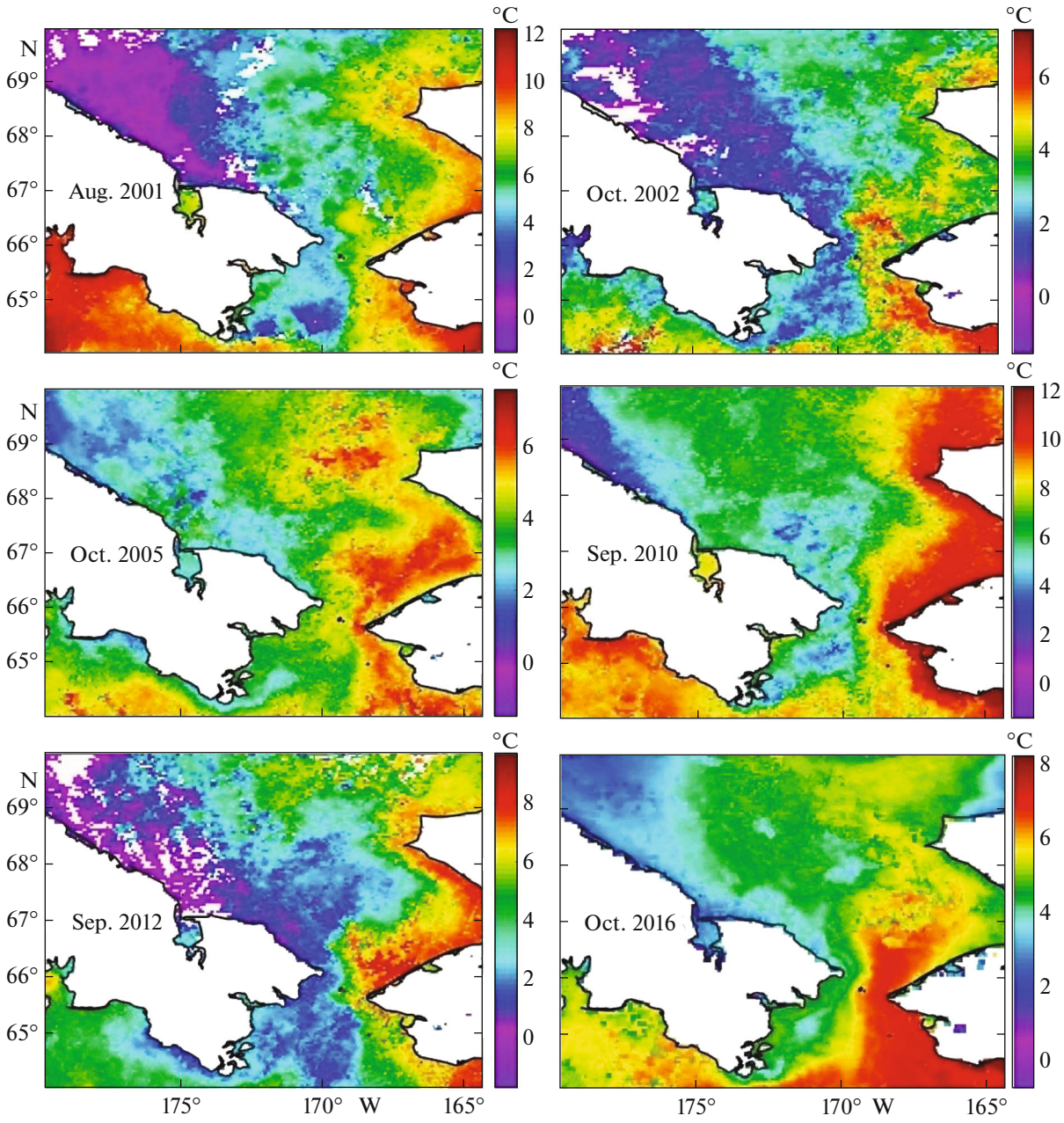

Fig. 7. Monthly mean temperature maps showing the penetration of cold waters of Arctic origin into the eastern part of the Bering Strait.

eastern component of the current velocity (Fig. 8). The time series were preliminarily smoothed with a 1-year running average to highlight the correlation on interannual time scales and filter out the seasonal variation.

High values of the inverse correlation coefficient of the northern currents with the eastern ones in the coastal area of the Chukchi Peninsula, where they reach 0.5–0.8, are clearly seen in Fig. 8. Thus, the results show that enhancement of transport across the strait is facilitated by weakening of the eastern velocity component near the southern coast of the Chukchi Sea. On the contrary, intensification of the East Siberian Current leads to a decrease in the northern current in the strait. The region of the greatest negative correlation is located to the west of the strait, in the eastern part of the Chukchi Peninsula with coordinates 66°–69° N, 178°–170° W.

The red line in Fig. 5 shows the variability of the eastern component of the velocity *Vx* over the section (shown in Fig. 8 by the purple line) corresponding to the position of the coastal East Siberian Current. As

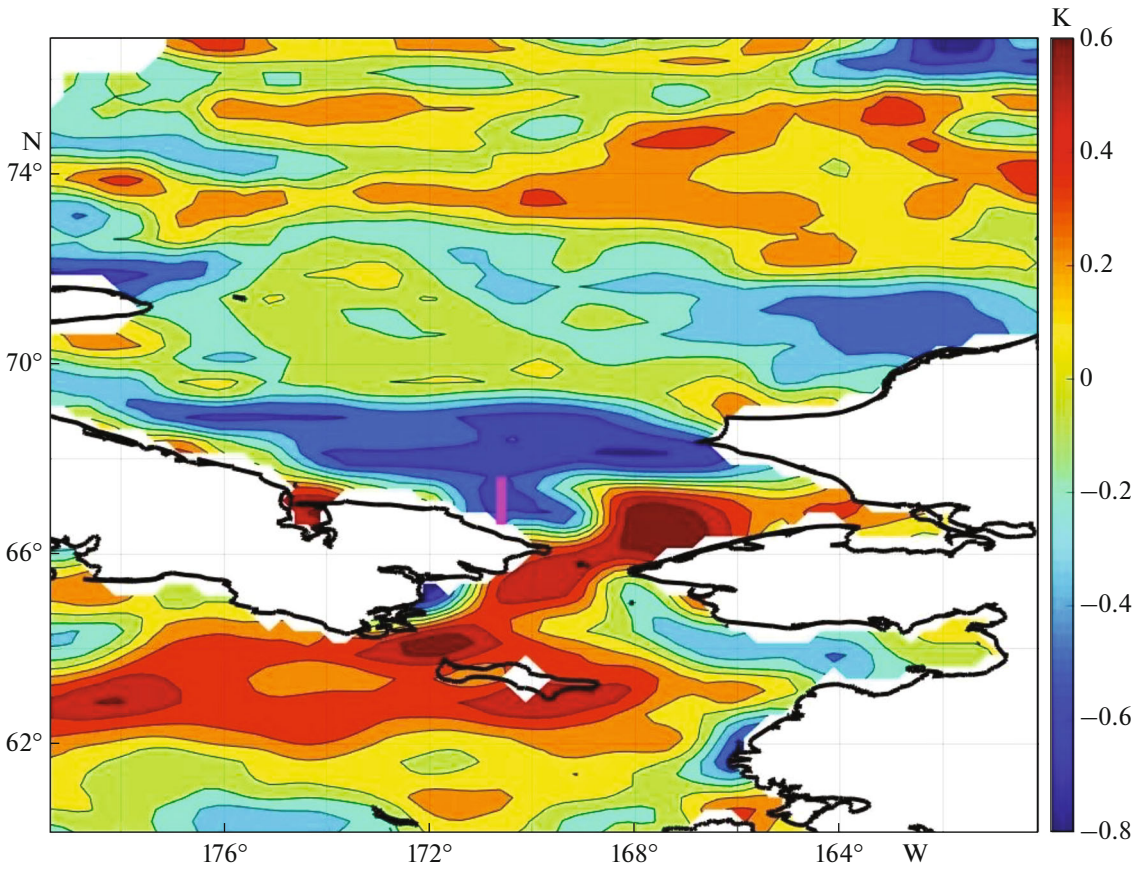

Fig. 8. Correlation of the mean meridional current velocity in the Bering Strait with the eastern component of the Chukchi Sea currents. The purple line indicates the section for study the velocity of the East Siberian Current.

can be seen from Fig. 5, an increase in the current velocity in this region in 2003–2004 and 2011–2013 contributed to a decrease in the flow of Pacific waters in the Bering Strait, while its weakening in 2006 and 2013–2014 caused an increase in this flow.

3.3. Influence of the Wind on the Interannual Variability of the East Siberian Current in the Bering-Strait Region

The results of the previous section show that as the East Siberian Current intensifies, it reaches the western part of the Bering Strait and causes a sharp change in the characteristics of water exchange. Thus, the dynamics of the East Siberian Current strongly modulates the inflow of Pacific waters into the Arctic.

To estimate the effect of wind on water exchange in the Bering Strait, a map of the correlation coefficient between water flow in the Bering Strait and the wind-speed components was constructed from the time series smoothed by a one-year filter (Fig. 9). On an interannual scale, the correlations are high not over the strait itself, but north of the New Siberian Islands. In the same region, the authors of recent works found the strongest relationship between the sea level and flow through the Bering Strait based on the data of gravimetric [14] and model [13] measurements. Analysis of the correlation map shows that intensification of the northwestern winds, or rather, weakening of the southeastern winds prevailing in this region, causes an increase in the flows through the Bering Strait.

A branch of the eastern current transporting Atlantic waters into the East Siberian Sea is located in this region. The quasi-permanent coastal East Siberian Current is formed as a result of the interaction of density currents formed by the runoff of the Lena River and a number of other small rivers into the East Siberian Sea, and wind action [24]. It is capable of changing its direction from the southeast to the northwest and mixing with the Pacific waters when it deviates from the coast [12]. The current deviates from the coast at a point, which appears when the coastal pressure gradient disappears and changes synoptically and seasonally [24, 27].

The northwestern winds induce Ekman transport directed by 60° to the right, thus facilitating the transport of fresh river water to the west [4, 11]. As a result, the transport of river waters in the direction of the strait weakens. The absence of salinity gradients associated with this transport leads to weakening and separation of the East Siberian Current from the coast.

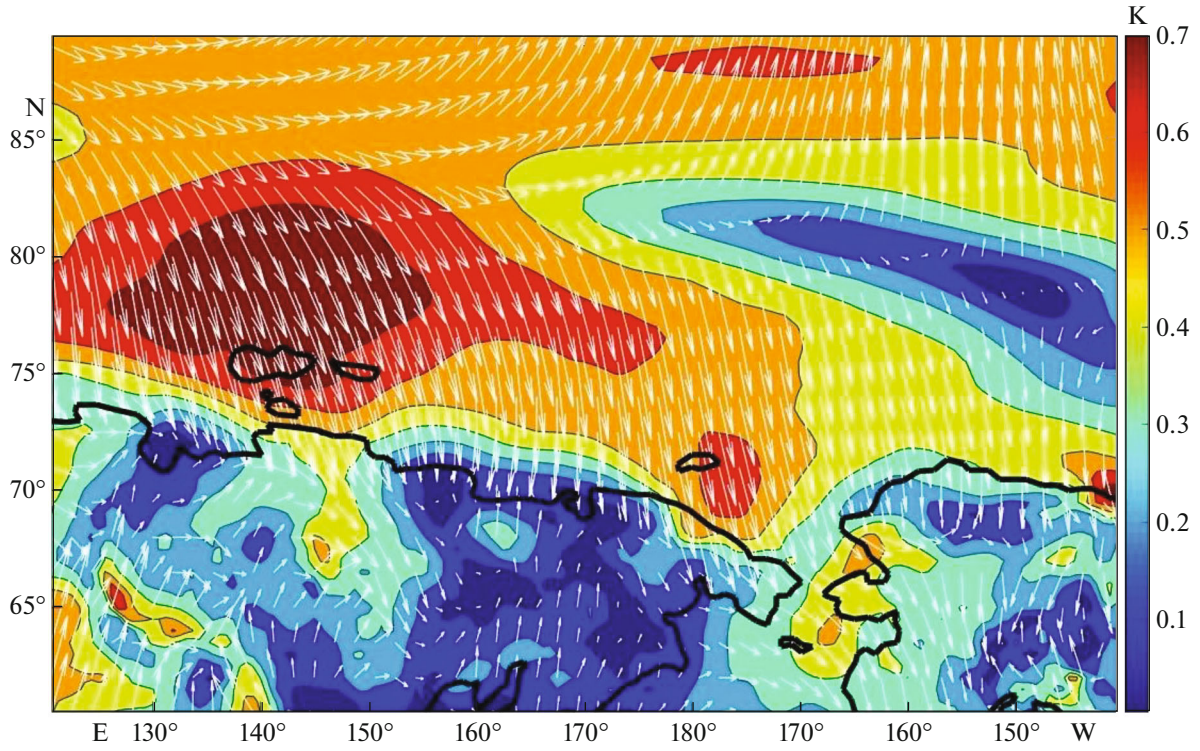

Fig. 9. Correlation of the mean meridional current velocity in the Bering Strait with the wind direction.

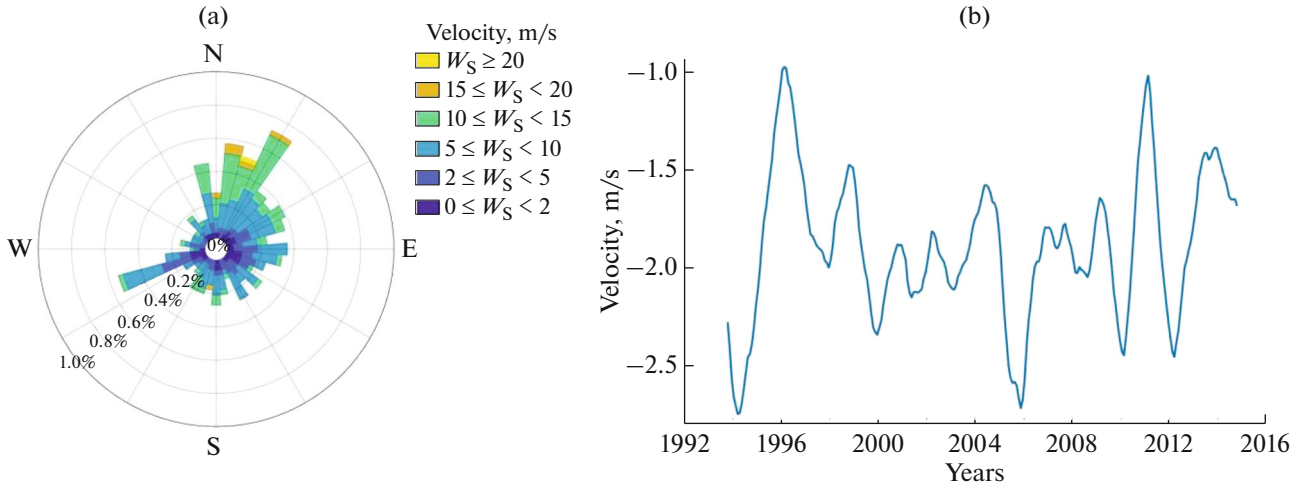

Fig. 10. Wind rose over the Bering Strait over the entire observation period (a). Interannual variability of the meridional wind speed component (negative values are related to the northern wind) over the strait smoothed by a 1-year running average (b).

Thus, it does not reach the strait, which enhances the flow of Pacific waters to the north. On the contrary, the southeastern winds cause intensification of the eastern transport of desalinated waters, intensification of the East Siberian Current, and its flowing into the strait.

The correlation between the flow of Pacific waters and the wind speed directly over the strait on interannual scales is much lower (the correlation coefficient is approximately 0.3–0.4, Fig. 9). Thus, the variability of the local wind speed has a significantly smaller effect on the geostrophic speed in the strait than the effect of distant winds over the East Siberian Sea. At the same time, local winds can cause intense barotropic drift currents that cannot be estimated from altimeters. Figure 10a shows a wind rose over the strait based on the Quikscat data. On average, the wind speed is low

and amounts to about 6.4 m/s. Over the strait, the winds are predominantly directed south against the flow of Pacific waters. The short-term variability of the wind is very high and is capable of causing abrupt rapid changes in the speed in the strait [27]. However, on interannual scales, the velocity component *Vy* changes insignificantly: from –0.16 to –2.77 m/s (Fig. 10b).

4. CONCLUSIONS

The flows of Pacific waters through the Bering Strait have a major impact on the biological and hydrological regimes of the entire Arctic Ocean. In this work, the intra-annual and interannual variability of water exchange in the Bering Strait in the period 1993–2016 has been investigated for the first time on the basis of satellite-altimetry data. The results are in good agreement with the data of contact measurements [25, 26], showing an increase in currents in summer and a weakening in autumn. At the same time, the altimetry data indicate that intense southern geostrophic currents can periodically appear in the strait in the autumn period with velocities up to 30 cm/s.

It is shown that the main features of water-exchange variability are the presence of sharp minima in 2002–2003 and 2012–2013, when the mean velocity decreased by more than 1.5 times. On the basis of the analysis, the relationship between the flows of Pacific waters through the Bering Strait and the intensity of the East Siberian Current has been substantiated. It is shown that the periods of weakening of the total flow through the strait are associated with intensification of this current, which in some years flows into the strait and causes a southern current in its western part. As a result, the East Siberian Current partially blocks the inflow of Pacific waters, the width and intensity of the flow of which into the Arctic is weakening. Such a bi-directional structure of currents in the Bering Strait is also well observed from satellite measurements of the surface temperature, which periodically record the penetration of cold Arctic waters into the eastern part of the Bering Strait in autumn. Analysis showed that intensification of the southeastern winds north of the New Siberian Islands, which apparently leads to an increase in the eastern transport of waters from the Laptev Sea, causes intensification of the East Siberian Current on an interannual scale and its penetration into the Bering Strait.

These results demonstrate that it is precisely the Arctic circulation, or rather the dynamics of the East Siberian Current, that primarily controls the water exchange between the Arctic and the Pacific Ocean, periodically leading to a significant decrease in the transport of Pacific waters through the strait.

FUNDING

The study of the variability of water exchange through the Bering Strait was supported by the state assignment 0555-2021-0006. Analysis of the relationship between water exchange and the dynamics of the East Siberian Current was supported by the Russian Science Foundation, grants 21-77-10052 and 21-17-00278.

REFERENCES

1. E. O. Basyuk, G. V. Khen, and N. S. Vanin, "Variability of the oceanological conditions of the Bering Sea in 2002–2006," Izv. Tikhookean. Nauchno-Issled. Inst. Rybn. Khoz. Okeanogr. **151**, 290–311 (2007).
2. A. D. Dobrovol'skii and B. S. Zalogin, *The Seas of the USSR* (Moscow State Univ., Moscow, 1982) [in Russian].
3. E. A. Zakharchuk and N. A. Tikhonova, "Intensity of currents of different time scales in the Chukchi Sea and Bering Strait," Russ. Meteorol. Hydrol., No. 1, 58–66 (2006).
4. A. G. Zatsepin, V. V. Kremenetskiy, A. A. Kubryakov, et al., "Propagation and transformation of waters of the surface desalinated layer in the Kara Sea," Oceanology (Engl. Transl.) **55**, 450–460 (2015). https://doi.org/10.1134/S0001437015040153
5. A. G. Andreev, M. V. Budyansky, G. V. Khen, and M. Y. Uleysky, "Water dynamics in the western Bering Sea and its impact on chlorophyll a concentration," Ocean Dyn. **70**, 593–602 (2020). https://doi.org/10.1007/s10236-020-01347-7
6. E. T. Brugler, R. S. Pickart, G. W. K. Moore, et al., "Seasonal to interannual variability of the Pacific water boundary current in the Beaufort Sea," Prog. Oceanogr. **127**, 1–20 (2014).
7. J. Y. Cherniawsky, W. R. Crawford, O. P. Nikitin, and E. C. Carmack, "Bering Strait transports from satellite altimetry," J. Mar. Res. **63** (5), 887–900 (2005). https://doi.org/10.1357/002224005774464201
8. B. W. Corlett and S. P. Robert, "The Chukchi slope current," Prog. Oceanogr. **153**, 50–65 (2017). https://doi.org/10.1016/j.pocean.2017.04.005
9. S. L. Danielson, T. J. Weingartner, K. S. Hedstrom, et al., "Coupled wind-forced controls of the Bering-Chukchi shelf circulation and the Bering Strait throughflow: Ekman transport, continental shelf waves, and variations of the Pacific-Arctic sea surface height gradient," Prog. Oceanogr. **125**, 40–61 (2014). https://doi.org/10.1016/j.pocean.2014.04.006
10. Y. Faugere, F. Mertz, and J. Dorandeu, Envisat validation and cross calibration activities during the verification phase, 2003. https://earth.esa.int/documents/700255/702255/ENVISAT_Verif_Phase_CLS.pdf/c3f76159-679c-4d13-bb9c-7cb9107b0c79?version=1.0.
11. A. A. Kubryakov, S. V. Stanichny, and A. G. Zatsepin, "River plume dynamics in the Kara Sea from altimetry-based lagrangian model, satellite salinity and chlorophyll data," Remote Sens. Environ. **176**, 177–187 (2016). https://doi.org/10.1016/j.rse.2016.01.020
12. A. Münchow, T. J. Weingartner, and L. W. Cooper, "The summer hydrography and surface circulation of the East Siberian Shelf Sea," J. Phys. Oceanogr. **29** (9), 2167–2182 (1999). https://doi.org/10.1175/1520-0485(1999)029<2167:TSHASC>2.0.CO;2

13. A. T. Nguyen, R. A. Woodgate, and P. Heimbach, "Elucidating large-scale atmospheric controls on Bering Strait throughflow variability using a data-constrained ocean model and its adjoin," J. Geophys. Res.: Oceans **125** (9), (2020). https://doi.org/10.1029/2020JC016213
14. C. Peralta-Ferriz and R. A. Woodgate, "The dominant role of the East Siberian Sea in driving the oceanic flow through the Bering Strait—Conclusions from GRACE ocean mass satellite data and in situ mooring observations between 2002 and 2016," Geophys. Res. Lett. **44** (22), 11472–11481 (2017). https://doi.org/10.1002/2017GL075179
15. S. V. Prants, A. G. Andreev, M. Yu. Uleysky, and M. V. Budyansky, "Lagrangian study of mesoscale circulation in the Alaskan Stream area and the eastern Bering Sea," Deep Sea Res., Part II **169**, 104560 (2019). https://doi.org/10.1016/j.dsr2.2019.03.005
16. M. H. Rio, S. Guinehut, and G. Larnicol, "New CNES-CLS09 global mean dynamic topography computed from the combination of GRACE data, altimetry, and in situ measurements," J. Geophys. Res.: Oceans **116** (7), (2011). https://doi.org/10.1029/2010JC006505
17. M. H. Rio, S. Mulet, and N. Picot, "New global mean dynamic topography from a GOCE geoid model, altimeter measurements and oceanographic in-situ data," in *Proceedings of the ESA Living Planet Symp., Edinburgh, September 9–13, 2013* (Edinburgh, 2013), No. ESA SP-722. ISBN 978-92-9221-286-5. https://ftp.space.dtu.dk/pub/Ioana/papers/s211_2rio.pdf.
18. A. T. Roach, K. Aagaard, C. H. Pease, et al., Direct measurements of transport and water properties through the Bering Strait," J. Geophys. Res.: Oceans **100** (9), 18443–18458 (1995).
19. M. C. Serreze, A. P. Barrett, A. D. Crawford, and R. A. Woodgate, "Monthly variability in Bering Strait oceanic volume and heat transports links to atmospheric circulation and ocean temperature, and implications for sea ice conditions," J. Geophys. Res.: Oceans **124** (12), 9317–9337 (2019). https://doi.org/10.1029/2019JC015422
20. M. Steele, J. Zhang, and W. Ermold, "Mechanisms of summertime upper Arctic Ocean warming and the effect on sea ice melt," J. Geophys. Res.: Oceans **115** (11), (2010). https://doi.org/10.1029/2009JC005849
21. D. L. Volkov and M.-I. Pujol, "Quality assessment of a satellite altimetry data product in the Nordic, Barents, and Kara seas," J. Geophys. Res.: Oceans **117** (3), (2012). https://doi.org/10.1029/2011JC007557
22. J. J. Walsh, C. P. McRoy, L. K. Coachman, et al., "Carbon and nitrogen cycling within the Bering/Chukchi Seas: source regions for organic matter effecting AOU demands of the Arctic Ocean," Prog. Oceanogr. **22** (4), 277–359 (1989). https://doi.org/10.1016/0079-6611(89)90006-2
23. T. Weingartner, K. Aagaard, R. Woodgate, et al., "Circulation on the north central Chukchi Sea shelf," Deep Sea Res., Part II **52** (24–26), 3150–3174 (2005). https://doi.org/10.1016/j.dsr2.2005.10.015
24. T. J. Weingartner, S. Danielson, Y. Sasaki, et al., "The Siberian Coastal Current: a wind and buoyancy-forced Arctic coastal current," J. Geophys. Res.: Oceans **104** (12), 29697–29713 (1999). https://doi.org/10.1029/1999JC900161
25. R. A. Woodgate, "Increases in the Pacific inflow to the Arctic from 1990 to 2015, and insights into seasonal trends and driving mechanisms from year-round Bering Strait mooring data," Prog. Oceanogr. **160**, 124–154 (2018). https://doi.org/10.1016/j.pocean.2017.12.007
26. R. A. Woodgate, K. Aagaard, and T. Weingartner, "Monthly temperature, salinity, and transport variability of the Bering Strait through flow," Geophys. Res. Lett. **32** (4), (2005). https://doi.org/10.1029/2004GL021880
27. R. A. Woodgate, K. M. Stafford, and F. G. Prahl, "A synthesis of year-round interdisciplinary mooring measurements in the Bering Strait (1990–2014) and the RUSALCA years (2004–2011)," Oceanography **28** (3), 46–67 (2015). https://doi.org/10.5670/oceanog.2015.57
28. R. A. Woodgate, T. Weingartner, and R. Lindsay, "The 2007 Bering Strait oceanic heat flux and anomalous Arctic sea-ice retreat," Geophys. Res. Lett. **37** (1), (2010). https://doi.org/10.1029/2009GL041621
29. R. A. Woodgate, T. J. Weingartner, and R. Lindsay, "Observed increases in Bering Strait oceanic fluxes from the Pacific to the Arctic from 2001 to 2011 and their impacts on the Arctic Ocean water column," Geophys. Res. Lett. **39**, (2012). https://doi.org/10.1029/2012GL054092
30. P. L. Woodworth and D. E. Cartwright, "Extraction of the M2 ocean tide from SEASAT altimeter data," Geophys. J. R. Astron. Soc. **84** (2), 227–255 (1986). https://doi.org/10.1111/j.1365-246X.1986.tb04355.x

Translated by E. Morozov